

Nonlinear vs. Linear Mesoscale Dynamics

G. Leoncini* and R. A. Pielke Sr.

Dept. of Atmospheric Science, Colorado State University, Fort Collins, Colorado

Introduction

The numerical integration of the full Navier-Stokes equations is notoriously expensive and its computational cost limits the ability to produce reliable fine spatial-scale real-time or near real-time weather forecasts. This problem can be partially overcome with the use of specialized models. For example if a particular situation, or weather pattern for a specific location, is known to be well approximated by a linear model, then it is possible to use an analytical solution which has the advantage of being exact and runs considerably faster. Another possibility, with similar advantages, is to use an analytical solution for the linear component and integrate numerically only the nonlinear one. This approach already proved successful for the shallow water equation (Weidman and Pielke, 1983). A third possible application consists in knowing whether the atmosphere is prevalently hydrostatic, because in this case pressure and temperature profiles can easily and quickly be obtained from each other, increasing the importance of remote sensing observations of one or the other variable. With these applications in mind the relevance of several terms in the equations which simulate mesoscale dry flow equations are investigated over a wide range of temporal and spatial scales, within the framework of Dalu et al. (2003). Specifically a modified version of the Regional Atmospheric Modeling System is used to compute the individual terms of advection, Coriolis effect, buoyancy, and dynamical pressure, as they appear in the Laplacian of the geopotential for the cases of linearized advection and fully nonlinear advection. In both cases, the atmosphere is forced with the same sensible heat fluxes. The main goal of this work is to verify that dynamic pressure and advection of buoyancy are responsible for most of the differences between the linear and nonlinear evolution of the flow.

The Equations

Following the Dalu et al. framework, here we illustrate the terms of the Poisson equation for the geopotential as obtained from RAMS equations, highlighting similarities and differences with Dalu et al., who studied a simpler set of equations. As in Rotunno (1983) the geopotential is defined as: $\phi = \theta_0 \pi$, where π is the perturbation Exner function, and θ_0 is the background potential temperature, horizontally homogeneous and constant in time. Then the RAMS mesoscale momentum equations can be written as:

$$\begin{aligned} T_x u &= f v - \theta \frac{\partial \pi}{\partial x} = f v - \left(1 + \frac{b}{g}\right) \frac{\partial \phi}{\partial x} \\ T_y v &= -f u - \theta \frac{\partial \pi}{\partial y} = -f u - \left(1 + \frac{b}{g}\right) \frac{\partial \phi}{\partial y} \\ T_z w &= g \frac{\theta - \theta_0}{\theta_0} - \theta \frac{\partial \pi}{\partial z} = b - \left(1 + \frac{b}{g}\right) \frac{\partial \phi}{\partial z} + \Gamma_0 \pi \end{aligned}$$

where b is the buoyancy, π the perturbation Exner function, θ the total potential temperature, f the Coriolis parameter, and Γ_0 the environmental lapse rate. Finally, T_x , T_y , and T_z are the components of the operator T

$$\vec{T} = \frac{\partial \vec{u}}{\partial t} + (\vec{u}_0 \cdot \nabla) \vec{u} - \nabla \cdot (K \nabla \vec{u})$$

and u_0 is equal to u for the nonlinear case and is held constant for the linear case. More specifically u_0 and v_0 are set to the background wind, and w_0 to zero, although w was used to compute the vertical advection of buoyancy. It is then easy to obtain the Poisson equation for ϕ :

$$\nabla^2 \phi = -\frac{1}{B} \left[\nabla \cdot (\vec{T} \vec{u}) - b_z - f(v_x - u_y) + \beta \bar{u} \right] + \frac{1}{B^2 g} \left[(\vec{T} \vec{u} \cdot \vec{\nabla}) \cdot b - f(v b_x - u b_y) - b b_z \right] + \pi \theta_{0z} + \pi_z \theta_{0z}$$

where subscripts represent derivatives, and B and β are defined as:

$$B = 1 + \frac{b}{g} \quad \beta = \frac{df}{dy}$$

It is important to notice that the difference between the linear and nonlinear advection case is entirely due to the different form of the operator T . The first term in T is the divergence of the acceleration, and it can be further decomposed into three parts (see the equation below). First the tendency of the velocity divergence, which is null in an incompressible atmosphere, then the divergence of the turbulent acceleration, and the divergence of the advection. This last term is a more general version of the Dalu et al. (2003) dynamic pressure.

$$\nabla \cdot (\vec{T} \vec{u}) = \frac{\partial}{\partial t} (\nabla \cdot \vec{u}) - \nabla \cdot [\nabla \cdot (K \nabla \vec{u})] + \nabla \cdot [(\vec{u} \cdot \nabla) \vec{u}]$$

The other term in T , in the Poisson equation, is due to the advection of buoyancy, and also has a corresponding term in Dalu et al. (2003). The second and third term of the Poisson also have an identical term in Dalu et al. (their Eq. 32) and represent the direct effect of buoyancy on the geopotential, and Coriolis effect, respectively. The fourth term ($\beta \bar{u}$) was not present in Dalu et al. since they assumed an f -plane. The second and third term of the second square bracket do not appear in Dalu et al., since they made the usual assumption that the potential temperature perturbation is negligible with respect to the control potential temperature perturbation. Here we have retained them since they derive their importance not from the absolute value of the perturbation, but from its spatial gradients. The last two terms originate from the rightmost one in the third momentum equation.

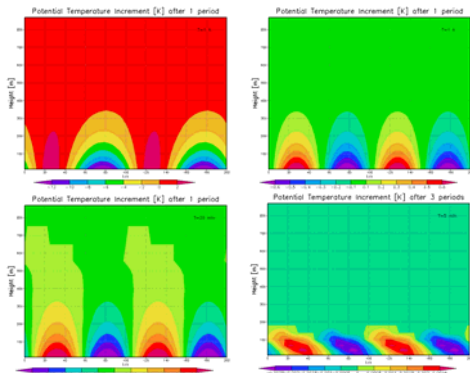


Fig. 1: Potential temperature increments for $L_x = 100$ km, linear advection, $u_0 = 0$ m s⁻¹.

Methodology

In order to retain as many similarities as possible with the Dalu et al. (2003) work and, at the same time to avoid boundary condition related issues, RAMS was forced only by periodic sensible heat flux exponentially decreasing with the height of the form:

$$Q = Q_0 \exp\left(-\frac{z}{L_z}\right) \cos\left(\frac{2\pi}{T}t + \frac{2\pi}{L_x}x + \frac{2\pi}{L_y}y\right)$$

Q_0 and L_z were both held constant for every simulation, and the respective values are 500 W m⁻², and 1000 m. To spin up the model fluxes ramped from zero to a cosine wave with the same maximum amplitude and wavelengths using a sine as the time factor. Duration of the spin-up was the shortest time between a quarter period and an hour. An important environmental parameter is the lapse rate which was 3 K km⁻¹, up to 1 km, and increasingly stable up to the tropopause. The vertical grid spacing was the same across all the simulations and had an initial Δz of 25 m, with a stretching of 1.12. The horizontal wavelengths L_x and L_y were always equal and were allowed two values: 100 and 10 km (indicated as L1 and L2). Initial tests demonstrated a significant sensitivity to resolution and grid spacing of one fortieth of the wavelengths were chosen, so that L1 and L2 simulations would have the same numerical representation of the wave. Domains encompassed two full wavelengths per side. Every simulation was carried out for the spin-up time and one period. The periods of the forcing used in the simulations were 6 h, 1 h, 20 min, and 5 min (A, B, C, and D). The background winds were always westerly of either 0 or 2.5 m s⁻¹ (u_0 , and u_2). Every configuration was also run with full and linear advection (FA, LA) as described in the introduction. During the simulations, all terms of the Poisson equations for ϕ are diagnosed, and the differences FA-LA are also evaluated, to at least estimate the different contribution to the nonlinear geopotential.

Results

The intensity of changes induced by the prescribed fluxes is strongly affected by the period of the forcing, since the time space integral of the fluxes, and therefore the energy first put into and the extracted from the system, are proportional to the product $L_x L_y T$, but the energy exchange per unit area is proportional to T . Furthermore a longer lasting source of energy gives wind and turbulence more time to advect and diffuse it. As shown in Fig. 1, as the energy exchanged increases, the temperature change at the end of the period increases in magnitude. The asymmetric pattern for the 6 h period simulation is due the turbulence that disperses the heat when the air is warmed, and to the decoupling of the atmosphere that sets when the air is cooled from the surface. The slanted warming-cooling pattern achieved by 5 minutes period forcing is due to its fast leftward movement, relatively to the time scale of turbulence that mixes the air. The intensity of the induced changes, though is so weak that the eight D simulations (L1Du0FA, L1Du2FA, L1Du0LA, and L1Du2FA, and L2 correspondent) are basically undifferentiated.

Quite surprisingly, given the analysis of Dalu et al. (2003), the main contributions to the nonlinear geopotential in all of the simulations come either from the change (i.e., the FA-LA difference) in vertical gradient of buoyancy (b_z) or from the change of the sum of the last two terms in the Poisson equation (herein addressed as "residual") and not the nonlinear convergence of mass and advection of buoyancy, which are orders of magnitude lower than the above mentioned changes. This is true for all our simulations, even when the velocities for the linear and nonlinear cases differ very little, that is to say where, according to Dalu et al., the nonlinear geopotential should differ from the linear case by the nonlinear convergence of mass and advection of buoyancy.

In this study, the vertical gradient of buoyancy is always the most important close to the surface, while the residual dominates the upper levels. The level where they switch relative importance changes with the period and wavelength of the forcing. If the period shortens, the fluxes inject less energy into the atmosphere and the level where b_z is not important, lowers. When the wavelength shortens the gradients steeper allowing stronger motions and a larger influence of b_z . More specifically the change in b_z is actually important only at the first model level above the ground (38 m) for both sets of simulations with a 5 m period forcing. On the other extreme, all of the 10 km wavelength runs with a 6 h period have b_z dominating the geopotential at all levels. The vertical gradient of buoyancy is also more important for the stronger wind simulations, and often the linear and nonlinear cases are indistinguishable when the background wind is zero.

Discussion and Conclusions

One reason, although minor, which could have led Dalu et al. (2003) to overestimate the importance of the nonlinear advection of buoyancy, and the nonlinear convergence of mass with respect to b_z , is the incompressibility assumption which generates stronger flows in response to vertical acceleration. Most likely our simulations have stronger values of b_z because of the different treatment of the vertical advection for the nonlinear case: they allow it only for the background potential temperature, whereas we allowed the full vertical advection of velocities and buoyancy.

The residual does not appear in Dalu et al. because in their third momentum equation, they neglected the term $\Gamma_0 \pi$. Generally, this is a good approximation for that equation, but taking one additional derivative to compute the Laplacian means to consider its vertical variations, which can behave differently.

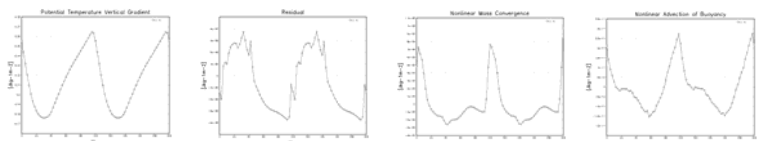


Fig. 2: Contributions to the geopotential difference between the nonlinear and linear cases for $L_x = 10$ km, $T = 1$ h, $u_0 = 2.5$ m s⁻¹ at $z = 12$ m.

References

- Dalu, G.A., M. Baldi, R.A. Pielke Sr., and G. Leoncini, 2003: Mesoscale nonhydrostatic and hydrostatic pressure gradient forces: Theory and parameterization. *J. Atmos. Sci.*, **60**, 2249-2266.
- Rotunno, R., 1983: On the linear theory of land and seabreeze. *J. Atmos. Sci.*, **40**, 1999-2009.
- Weidman, S.T. and R.A. Pielke, 1983: A more accurate method for the numerical solution of nonlinear partial differential equations. *J. Comput. Phys.*, **49**, 342-348.

Acknowledgment: This research is supported by the DoD Center for Geoscience/Atmospheric Research at Colorado State University under cooperative agreement DAAD19-02-2-0005 with the Army Research Laboratory.